Makara Journal of Technology

Volume 27 | Issue 3 Article 5

12-23-2023

# Effect of Lime Content, Curing Temperature, and Aging Condition on Low-Alkaline Concrete

Mahdi Parsa Pour
*Ayandegan Institute of Higher Education, Tonekabon 4681853617, Iran*

Reza Shaban Sharghi
*Ayandegan Institute of Higher Education, Tonekabon 4681853617, Iran*

Faezeh Nejati
*Ayandegan Institute of Higher Education, Tonekabon 4681853617, Iran*, civilinj1998@gmail.com

Elmira Khaksar Najafi
*Department of Civil Engineering, Faculty of Engineering, University of Guilan, Gilan 41625, Iran*



## Recommended Citation

Pour, Mahdi Parsa; Sharghi, Reza Shaban; Nejati, Faezeh; and Najafi, Elmira Khaksar (2023) "Effect of Lime Content, Curing Temperature, and Aging Condition on Low-Alkaline Concrete," *Makara Journal of Technology*: Vol. 27: Iss. 3, Article 5.
DOI: 10.7454/mst.v27i3.1527
Available at: https://scholarhub.ui.ac.id/mjt/vol27/iss3/5

Makara J. Technol. 27/3 (2023), 107–115
doi: 10.7454/mst.v27i3.1527

# Effect of Lime Content, Curing Temperature, and Aging Condition on Low-Alkaline Concrete

Mahdi Parsa Pour[1], Reza Shaban Sharghi[1], Faezeh Nejati[1*], and Elmira Khaksar Najafi[2]

1. Ayandegan Institute of Higher Education, Tonekabon 4681853617, Iran
2. Department of Civil Engineering, Faculty of Engineering, University of Guilan, Gilan 41625, Iran

*E-mail: nejati@aihe.ac.ir*

## Abstract

This study determines how curing temperatures, aging condition, and hydrated lime contents affect the unconfined compressive strength (UCS), modulus of elasticity, and workability of low-alkaline concrete. Samples were prepared in two different groups to determine the optimum hydrated lime content and aging conditions to assess the mutual effect of NaOH molarity and curing temperature, that is, 70 °C for 48 h or room temperature, on samples with and without lime. The results showed that the increase in hydrated lime content affected alkali concentration. The samples with lime exhibited a clear peak in UCS (6 M NaOH) compared with the continuous increase for the samples without lime. Lime content had a positive effect on eliminating heat curing and prolonging aging time to enhance the Young's modulus and compressive strength. This result is promising for in-situ concreting. Similar to the effect of alkali concentration, lime contributed to the loss in slump value. The scanning electron microscopy images showed the formation of N-(C)-A-S-H gels as the main reaction products. Moreover, internal cracking contributed to the lower UCS of samples with 9 M NaOH compared with those with 6 M NaOH.

*Keywords: fly ash, hydrated lime, in-situ concreting, low-alkaline concrete, unconfined compressive strength, workability*

## 1. Introduction

Alkaline cement has been introduced as a sustainable alternative to Portland cement to reduce the adverse environmental impacts of $CO_2$ emissions and energy and raw resource consumptions [1, 2]. Aluminosilicate gels, the main reaction products, are synthesized due to the reaction of amorphous aluminosilicate resources with highly concentrated hydroxide- or silicate-based solutions (typically Na or K) [3, 4]. Although alkaline cement shows superior mechanical performance to standard Portland cement, its full-scale production for in-situ concreting has been limited as it requires highly concentrated alkaline solutions and elevated temperatures to yield the final reaction products [1]. Highly concentrated alkaline solutions increase mixture viscosity and lead to decreased workability [5, 6], and elevated temperatures are not applicable for in-situ concreting. Alkaline cement shows superior mechanical strength that surpasses the requirements of many applications, such as construction materials and unreinforced concrete; therefore, a reduced dosage of the alkaline activator or recycling alkaline residues can increase the cost- and eco-efficiency of alkali-activated cement for geotechnical and structural applications [7]. Several studies applied presetting pressure to improve the mechanical and durability characteristics of low-alkaline cement [8, 9]. Gökçe *et al.* reported that presetting the pressure of fresh fly ash-based samples contributed to low porosity and thus high compressive strength. However, this altered construction is not applicable for in-situ concreting. Therefore, determining how a reduced alkali dosage can promote alkaline reactions in in-situ concreting where no preset pressure and elevated temperatures are accessible and applicable is essential. In addition, alkaline cement can be upgraded for in-situ concreting by introducing concentration limit in cement cured at ambient temperature.

For fly ash-based geopolymers, incorporating 12 M NaOH resulted in a high flexural strength of 10.119 MPa; however, a very high NaOH molarity may adversely affect the reaction products because of excessive $OH^-$ ions [10]. Similarly, Gebregziabiher *et al.* and Nejati *et al.* showed that excessive alkaline content does not contribute to a high mechanical strength [11, 12]. Álvarez-Ayuso *et al.* and Hooshmand *et al.* reported an optimum NaOH molarity of 8 M for fly ash class F, characterized by a low degree of reaction; excessive NaOH concentration up to 12 *M* contributed to a loss in UCS [13, 14]. However, in the same study, fly ashes with high reactivity showed a continuous rise in UCS due to the increased NaOH concentration. K. Chiranjeevi Reddy *et al.* reported a threshold of NaOH molarity for alkali-activated slag and stated that an increase in NaOH molarity from 1 to 3 M contributed to a considerably increase in compressive strength, but further increase in NaOH concentration led

to an insignificant rise in compressive strength [7]. These observations showed that the optimal NaOH concentration may be affected by the reactivity of the precursors and governed by material properties and curing temperature [15–17]. Slag-based alkali-activated materials contribute to a high mechanical strength under low alkali contents and curing temperatures due to the availability of Ca [7]. In in-situ concreting at room temperature, a low NaOH molarity may be suitable to reach the required strength for precursors containing Ca. For this reason, high-Ca supplementary materials, including limestone ($CaCO_3$) and hydrated lime, have received attention for enhancing the properties of alkali-activated materials [18, 19]. Hydrated lime is more effective than limestone in reducing drying shrinkage [20] and benefits alkaline cement by increasing alkaline and calcium contents. In addition, adding hydrated lime reduces drying shrinkage, enhances early age mechanical properties, and increasing autogenous shrinkage. Furthermore, lime is accessible and cost-friendly and can thus reflect the environmentally friendly aspects of alkaline cement [18]. Therefore, hydrated lime can be a suitable supplementary material to render eco-efficient in-situ concrete with low-dosage alkaline activation and ambient curing.

The primary objective of this study is evaluating the effect of curing temperature, aging condition, and hydrated lime content on low-alkaline concrete by measuring unconfined compressive strength (UCS) and workability. Two different groups of precursors, namely, pure fly ash and a mixture of fly ash and hydrated lime, were used. Different alkaline activators were implemented, and various NaOH concentrations of 3, 6, and 9 M were used to evaluate the effect of NaOH molarity. To analyze aging conditions and curing temperatures, samples were cured for the initial 48 h at 70 °C or room temperature, followed by aging in a dry or moist environment until testing. UCS, modulus of elasticity ($E_{60}$), workability and scanning electron microscopy (SEM) were analyzed to evaluate the effect of curing temperature, aging condition, and hydrated lime content on low-alkaline concrete.

## 2. Materials and Methods

**Materials.** Used aggregates were collected from the bed of the Cheshmeh Kileh River in Tonekabon County, Iran. Figure 1b demonstrates that the particle size distribution of the used sand lies between the low and high limits stated in ASTM C33 [21]. Meanwhile, Figure 1a displays

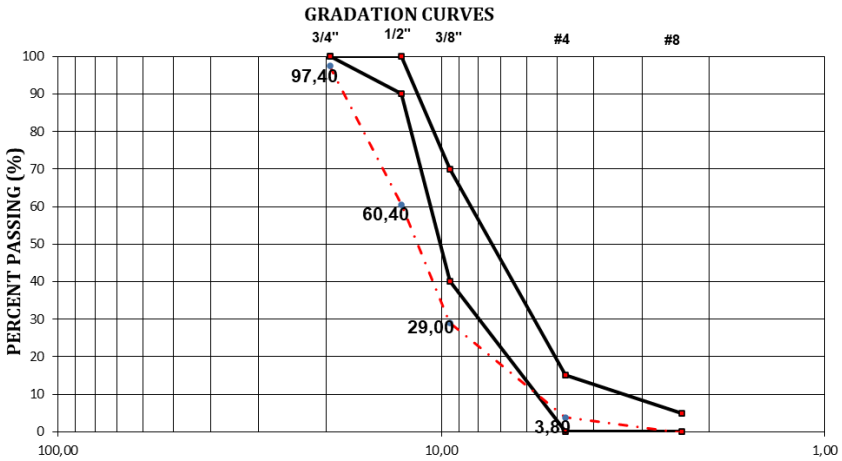


(a)

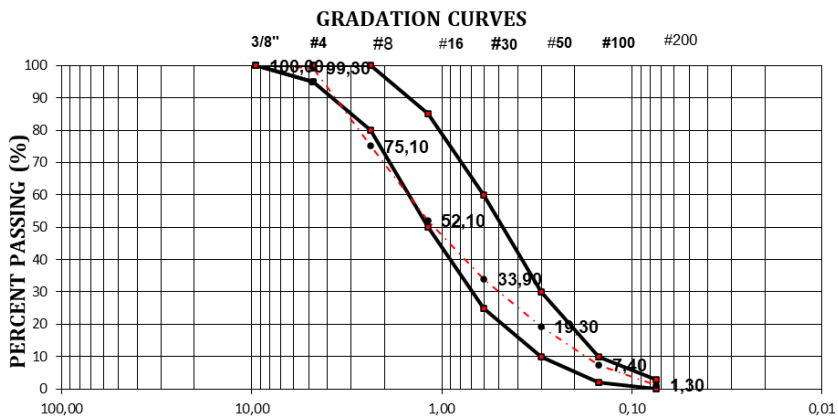


(b)

**Figure 1. Particle Size Distribution Curves of (a) Gravel and (b) Sand**

that the used gravel is coarser than the particle size specified in ASTM 33 [21]. Moreover, the used sand with a fineness modulus of 2.6 satisfies the criteria of ASTM C33 (2.3–3.1) [21]. The saturated surface-dry values of the fine and coarse aggregates obtained from ASTM C128 and C127 are 3.57 and 2.82, respectively [22, 23].

Fly ash class F ($FA_F$) and hydrated lime ($Ca(OH)_2$) were used as precursor and supplementary materials, respectively, for alkaline cement. Table 1 shows their chemical compositions obtained by x-ray fluorescence. $FA_F$ is the product of the power plants located in India, and hydrated lime was produced by an Iranian company located in Kerman City. The chemical composition of $FA_F$ indicated that it is a low calcium precursor and satisfies the chemical requirements of ASTM C618 [24]. Figure 2 presents the crystalline phases in the used fly ash, mullite, and quartz. To prepare the alkaline activator, 99% pure NaOH pellets were dissolved in distilled water and cooled down in room temperature. NaOH solutions with concentrations of 3, 6 and 9 M were used as the alkaline activator.

**Table 1. Chemical Components (wt.%) of Used Fly Ash and Hydrated Lime**

| Components | $FA_F$ | Lime |
|---|---|---|
| **$SiO_2$** | 61.10 | 0.5 |
| **$Al_2O_3$** | 28.97 | 0.5 |
| **$Fe_2O_3$** | 3.98 | 1 |
| **CaO** | 0.83 | 90 |
| **$Na_2O$** | 0.11 | - |
| **$K_2O$** | 0.99 | - |
| **MgO** | 0.44 | 1.5 |
| **$SO_3$** | - | 0.5 |
| **$TiO_2$** | 2.08 | - |
| **MnO** | 0.04 | - |
| **$P_2O_5$** | 0.318 | - |
| **LOI[b]** | 1.886 | 3.13 |

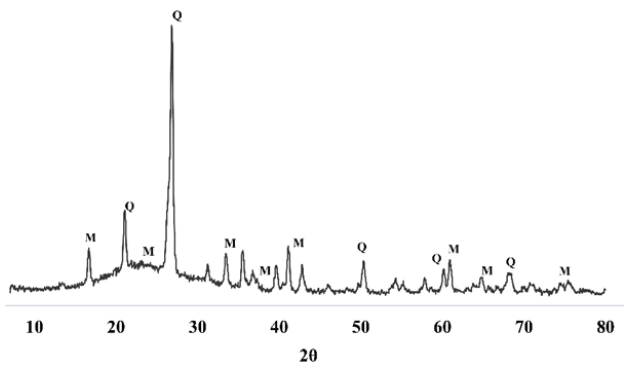


**Figure 2. X-ray Diffraction Patterns of the Raw Materials: M = Mullite, Q = Quartz**

**Mixing design and sample preparation.** As shown in Table 2, the mixture proportions used in this study were divided into two different groups. Groups 1 and 2 were prepared in four and two sets, respectively. Group 1 was used to determine the optimum hydrated lime percentage and aging condition, namely, dry or moist curing, after the initial 48 h of curing at 70 °C or room temperature, for a constant alkali content. Hydrated lime was added to fly ash as supplementary material at three different percentages, that is, 5%, 15%, and 30%, to determine the highest improvement induced by hydrated lime addition. Group 2 was used to assess the mutual effect of different alkali contents, that is, 3, 6, and 9 M NaOH, and initial 48 h of curing at 70 °C or room temperature, on the optimum hydrated lime content and aging condition obtained from Group 1. The ratios of aggregate/fly ash, activator/precursor, and sand/gravel were maintained as 4, 0.4, and 1, respectively, for all mixtures to eliminate the effect of water and aggregate content on the experimental results.

A concrete mixer was utilized to mix sand, gravel, fly ash, and hydrated lime with the alkaline activators. The mixing procedure was completed in approximately 8 min. The solid materials were first mixed at a slow speed for 3 min, and the alkaline solution was then gradually added into the mixture with additional mixing for another 5 min at a medium speed to ensure homogenous mixing without any dry materials remaining (Figure 3). Finally, the mixture was placed in three layers in one cubical mold (100 mm × 100 mm × 100 mm). Each layer was manually compacted by 25 strikes for air removal. For the next 24 h, the cast specimens were placed at room temperature (20 °C) and then remolded.

For Group 1, one set of each mixture was placed at room temperature and the second set was submerged until the testing day, that is, 7 days after preparation. The third and fourth sets of each mixture were subjected to heat curing at 70 °C for the first 48 h; one was stored in ambient temperature, and the other was submerged in water until the test day, that is, 7 days after preparation. Each set consisted of eight cubic samples to test compressive strength. For Group 2, one set of each mixture was placed at room temperature, and the second set was subjected to heat curing at 70 °C for the first 48 h and then stored in an ambient curing until the test days, namely, 7, 28, and 90 days after preparation. Each set consisted of 36 cubic samples for compressive tests. For each experiment, two identical samples were prepared.

**Experimental tests.** The workability of the fresh mixtures was measured promptly after preparing the paste for the slump cone test in accordance with ASTM C143 [25]. The sizes of the slump cone devices were 100, 200, and 300 mm. Each mixture was tested twice and the results were averaged. The compressive strength of the samples was measured using a digital testing machine

**Table 2. Details of the Mixtures' Proportions and the Experimental Program**

| | Samples | NaOH concentration (mol/L) | Gravel (gr) | Sand (gr) | Lime (gr) | Fly ash (gr) | Activator (gr) | UCS tests, curing period (days) | ITS test, curing period (days) | Aging condition | Initial 48 h curing temperature |
|---|---|---|---|---|---|---|---|---|---|---|---|
| Group 1 | **GPL0$_i$** | 6 | 900[a] | 900 | - | 450[b] | 180[c] | 7 | - | Dry/moist | room/70 ºC |
| | **GPL0.05$_i$** | 6 | 900 | 900 | 22.5 | 427.5 | 180 | 7 | - | Dry/moist | room/70 ºC |
| | **GPL0.15$_i$** | 6 | 900 | 900 | 67.5 | 382.5 | 180 | 7 | - | Dry/moist | room/70 ºC |
| | **GPL0.3$_i$** | 6 | 900 | 900 | 135 | 315 | 180 | 7 | - | Dry/moist | room/70 ºC |
| Group 2 | **GP3$_i$** | 3 | 900 | 900 | - | 450 | 180 | 7, 28, 90 | 90 | Dry | room/70 ºC |
| | **GPL3$_i$** | 3 | 900 | 900 | 67.5 | 382.5 | 180 | 7, 28, 90 | 90 | Dry | room/70 ºC |
| | **GP6$_i$** | 6 | 900 | 900 | - | 450 | 180 | 7, 28, 90 | 90 | Dry | room/70 ºC |
| | **GPL6$_i$** | 6 | 900 | 900 | 67.5 | 382.5 | 180 | 7, 28, 90 | 90 | Dry | room/70 ºC |
| | **GP9$_i$** | 9 | 900 | 900 | - | 450 | 180 | 7, 28, 90 | 90 | Dry | room/70 ºC |
| | **GPL9$_i$** | 9 | 900 | 900 | 67.5 | 382.5 | 180 | 7, 28, 90 | 90 | Dry | room/70 ºC |

a: Gravel/Sand ratio = 1, b: Aggregate/Precursor = 4, c: Activator/Precursor = 0.4, i = R or H, changing according to curing temperature, including room and heated temperature, respectively

**Figure 3. Prepared Mixture**

(manufactured by an Iranian Azmoon company) in accordance with ASTM C39 [26]. Compressive strength tests were conducted on Group 1 after curing for 7 days and Group 2 after curing for 7, 28, and 90 days to assess the effect of curing temperature, aging condition, and hydrated lime content on low-alkaline concrete. A set of two samples was tested at each indicated age and the experimental results were averaged out of two identical samples.

**Microstructural analysis.** Samples for mechanical compressive strength tests were prepared for microstructural analysis using SEM images. Mixtures GP6$_R$, GPL6$_R$, GPL9$_R$, GP6$_H$, GPL6$_H$, and GPL9$_H$ were selected to evaluate the effect of lime and alkali concentrations on the surface morphology of the concrete. SEM analyses were conducted with MIRA III on the specimens sputter-coated with a thin layer of gold.

## 3. Results and Discussion

**Compressive strength.** Figure 4 reveals that the samples containing 15% hydrated lime exhibited the highest UCS after 7 days of curing for all aging conditions. Regarding aging condition, dry environments worked better than wet environments for all samples. Therefore, 15% hydrated lime and dry environment were used to prepare the samples for Group 2. In line with findings in this study, Pacheco-Torgal, *et al*. reported an optimum value (10%) of $Ca(OH)_2$ that led to the highest compressive strength; a further increase in calcium hydroxide content contributed to a loss in UCS [27]. Likewise, Nath, *et al*. reported that the optimum amount of fly ash replacement by slag was 15% [28]. Adding calcium up to 15% favors the production of alkali-activated materials because the coexistence of N-A-S-H and C-A-S-H leads to high UCS [29]. Regarding aging condition, Ban, *et al.* and Khan, *et al.* showed that a moist environment contributed to a reduction in the mechanical strength of alkali-activated materials due to the reduction in the pH of the pore solution, which is essential for alkaline activation [30, 31]. As a consequence, the moist environment rendered a low UCS.

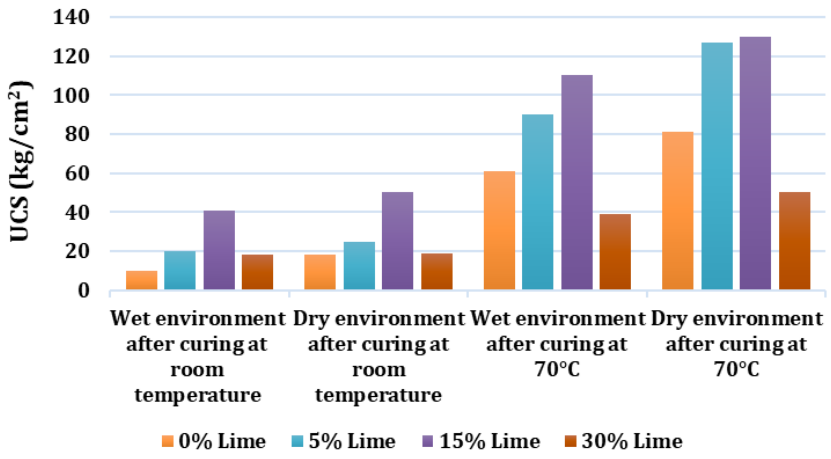


**Figure 4. Variation of Unconfined Compressive Strength Under Different Lime Contents and Aging Condition After the Initial 48 h of Curing at 70 °C or Room Temperature**

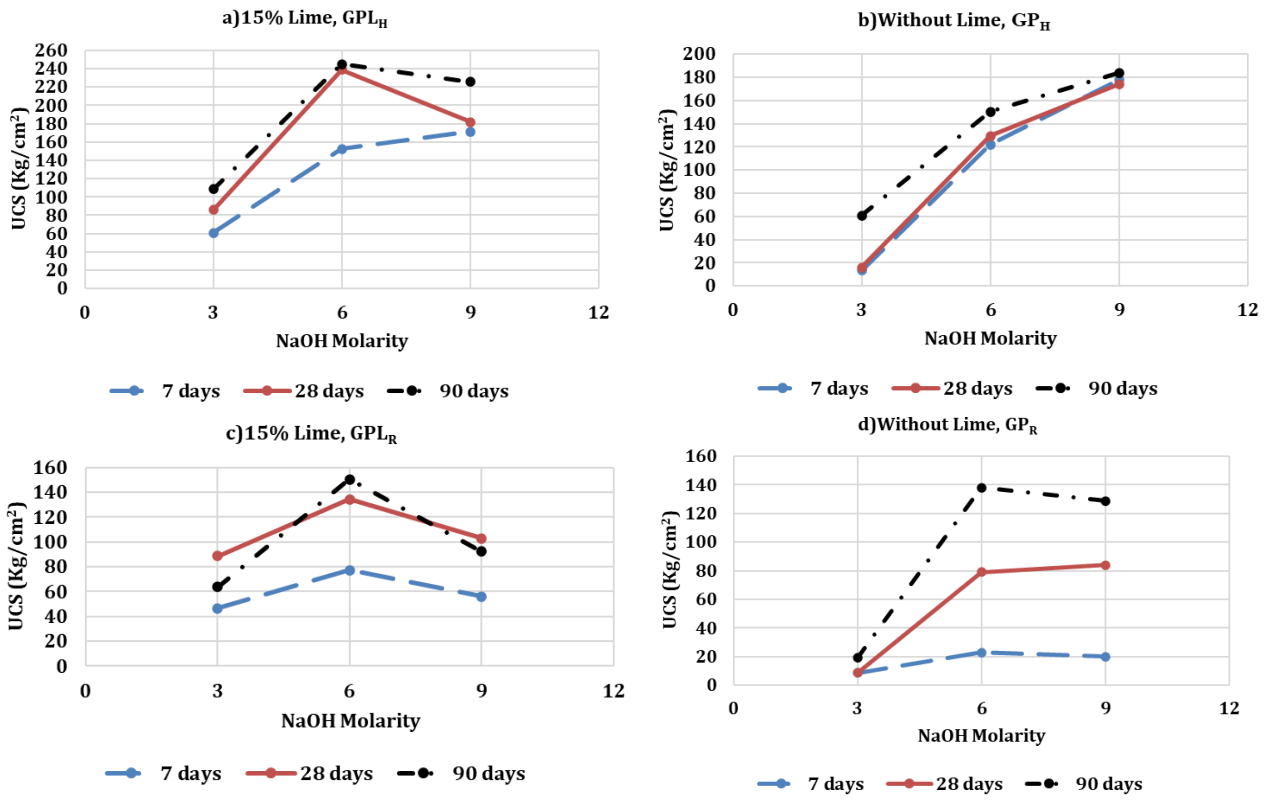


**Figure 5. Variation of UCS with NaOH Concentration: a) $GPL_H$, b) $GP_H$, c) $GPL_R$, and d) $GP_R$ after 7, 28, and 90 Days of Aging**

Irrespective of curing temperature, the samples with 15% hydrated lime showed clear peaks of USC when added with 6 M NaOH (Figures 5a and 5c). Meanwhile, the samples without hydrated lime cured at elevated and room temperatures (Figures 5b and 5d) exhibited a continuous rise and a slight drop in their UCS values, respectively, due to the increase in NaOH concentration to 9 M. However, the corresponding UCS values were lower than those of $GPL6_H$ and $GPL6_R$. Therefore, adding hydrated lime positively affects the performance of specimens with low NaOH concentration. NaOH at 6 M worked better than at 9 M, especially for heat curing. A high NaOH molarity leads to a highly alkaline environment, hindering the dissolution of calcium due to the large amount of $OH^-$ [32, 33]. K. Chiranjeevi Reddy, *et al.* also reported that an increase in NaOH concentration limited the formation of C-(A)-S-H in alkali-activated materials [7]. For precursors containing Ca, the early and

rapid dissolution of calcium in a low-alkaline environment led to the production of C-(A)-S-H gels [34, 35]. Owing to the availability of Na, N–(C)–A–S–H gels are then produced in the mixture after the consumption of calcium at the early stages. These gels complete each other and thus contribute to a dense structure with a high degree of cross-linking and improved mechanical behavior [36].

For curing temperature, heating improves and accelerates the reaction [37]. The specimens containing lime and cured at elevated temperatures exhibited the highest UCS for all three NaOH molarities and curing times. $GPL6_H$ showed the highest UCS of 250 *kg/cm²* at the age of 90 days, followed by GPL9 reaching 200 *kg/cm²* for the same curing period. Manjarrez *et al.* reported that a high curing temperature of 70 °C for 24 h contributed to the high strength of the geopolymer synthesized with 50% slag and 50% tailings [38].

$GPL6_R$, $GL6_H$, and $GL6_R$ reached almost equal UCS values of 150, 150, and 140 *kg/cm²* after 90 days of curing. Although $GL6_R$ showed an UCS of 140 *kg/cm²* UCS after 90 days of curing, either lime addition or heat curing reduced its curing time to 28 days to reach a UCS of 138 *kg/cm²*, which is satisfactorily above the minimum compressive strength specified in ASTM C90 [39] for normal-weight, load-bearing masonry units. $GPL6_H$ satisfies the minimum UCS of 250 *kg/cm²* for medium-weight concrete and the UCS of 150 *kg/cm²* for unreinforced foundation, boundary walls, and freestanding retaining walls [40]. An increase in calcium content and curing temperature increases the rate of chemical reactions, dissolution of reactive species, gel production, and early-age strength development; meanwhile, low curing temperature and calcium content require a long curing time [37, 41, 42]. In this study, the increase in hydrated lime content or curing temperature similarly increases the mechanical strength of the alkali-activated concrete and reduces the curing time to reach similar UCS. This finding is very useful for in-situ concreting, wherein adding lime eliminates the need for heat curing to achieve same UCS value.

**Stiffness (modulus of elasticity).** The modulus of elasticity (*E60*) was calculated using the stress–strain curves of the specimens obtained from the UCS tests, where the slope between the stress corresponding to 60% of the ultimate stress and the stress equivalent to a longitudinal strain of 0.00005 was determined according to ASTM C469 [43]. Figure 6 indicates that the variations in *E60* exhibited a similar trend to the compressive strength shown in Figure 5, where the maximum *E60* of 28,000 kg/cm² was recorded for $GPL6_H$. Similar to the trend for UCS, only a slight difference in *E60* was observed between $GPL6_R$ and $GP6_R$. Therefore, adding lime reduces the required aging time to reach the *E60* of 16,000 kg/cm², which is very important in filed applications.

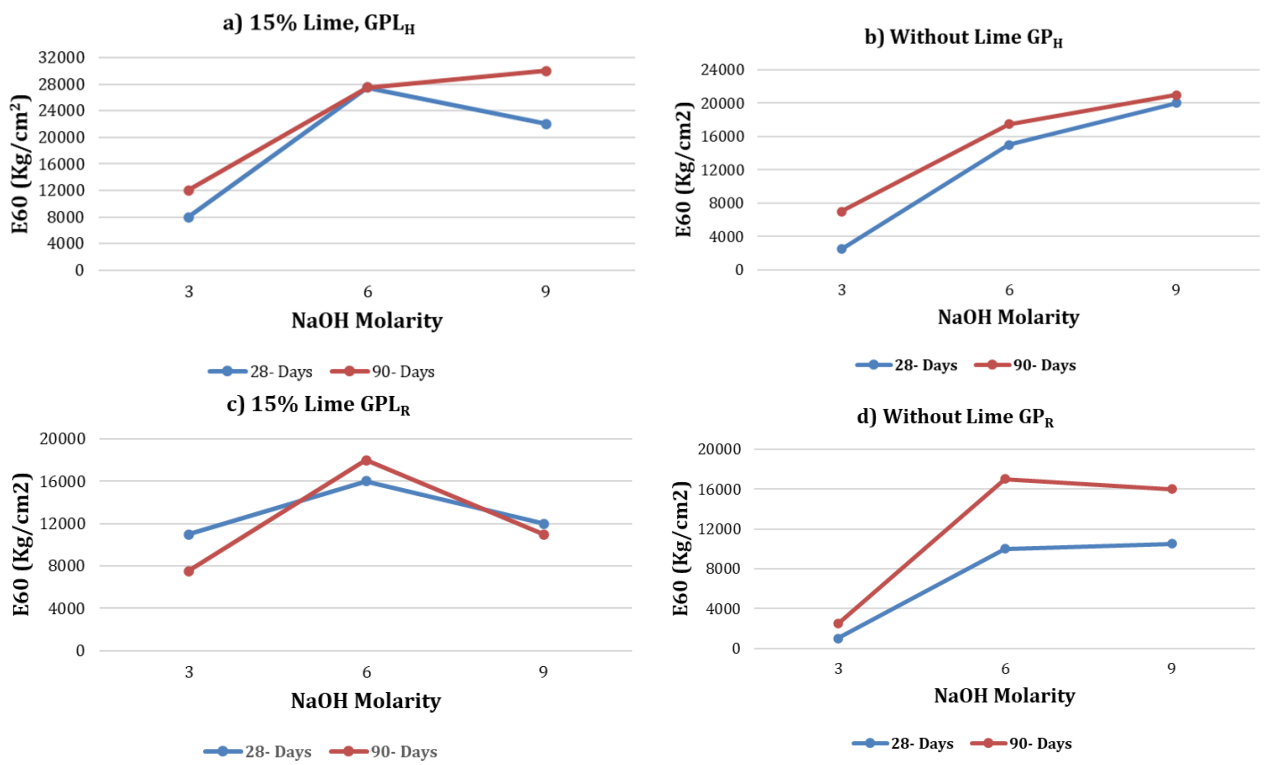


**Figure 6. Variation of E60 with NaOH Concentration: a) $GPL_H$, b) $GP_H$, c) $GPL_R$, and d) $GP_R$ after 28 and 90 Days of Aging**

**Workability.** The slump value of each sample is presented in Figure 7. The increase in alkali content contributed to a loss in slump value, with the value reducing from 3 to 2.5 due to the increase in alkali concentration from 3 to 9 M. Furthermore, the specimens containing hydrated lime exhibited a relatively low slump value primarily due to the fast reaction and solidification, providing nucleation sites for the precipitation of the aluminosilicate phases dissolved by calcium [31]. Similar to the effects of calcium, the increase in alkali concentration affects the slump value due to the rapid solidification and reaction [44].

**SEM analysis.** Figure 8 shows the SEM images of $GPL6_H$, $GP6_H$, $GPL6_R$, and $GP6_R$ after a curing period of 90 days. In line with mechanical results, $GPL6_H$ was more condensed and compacted with lower porosity compared with the other samples because it had the lowest amount of unreacted fly ash and due to the formation of many binding gels. A comparison between Figures 8a and 8b shows the higher amount of unreacted fly ash particles and high porosity for $GP6_H$ compared with $GPL6_H$. Similar comparisons and observations are valid for $GPL6_R$ and $GP6_R$, indicating that adding lime contributes to the compact and dense structure with low porosity of the samples cured at room temperature. The presence of partially dissolved fly ash in $GPL6_H$ was due to the effect of lime content and heating.

For the effect of curing temperature, $GPL6_R$ and $GPL6_H$ were covered by plate-like surfaces covered by irregular agglomerated amorphous passes, which may be attributed to N-(C)-A-S-H gels [45]. Figure 8a shows that $GPL6_H$ contained a flocculent morphology with low pore spaces. These differences were evident between $GP6_R$ and $GP6_H$, in which the former contained considerable pore spaces. In terms of the effect of lime contents, $GPL6_H$ and $GPL6_R$ exhibited a denser structure containing more flocculent morphology and less unreacted fly ash and pores, respectively, compared with $GP6_H$ and $GP6_R$. Like the observations made by Yang *et al.* and Nejati *et al.* for low-Na cement cured at a low temperature, the reaction products of $GP6_R$ were irregular amorphous N-A-S-H gels [46, 47].

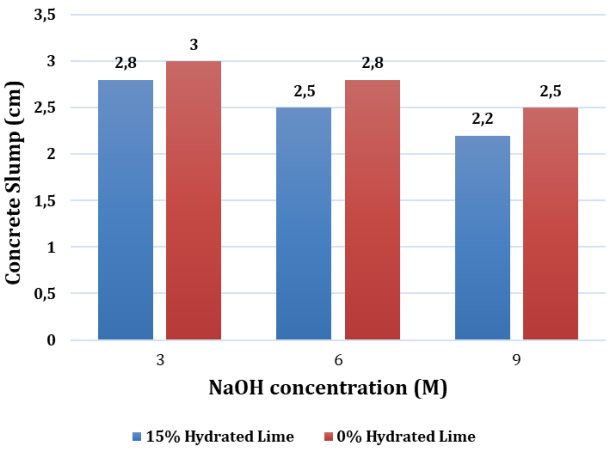


**Figure 7. Variation of Slump Values with NaOH Concentration for the Samples in Group 2**

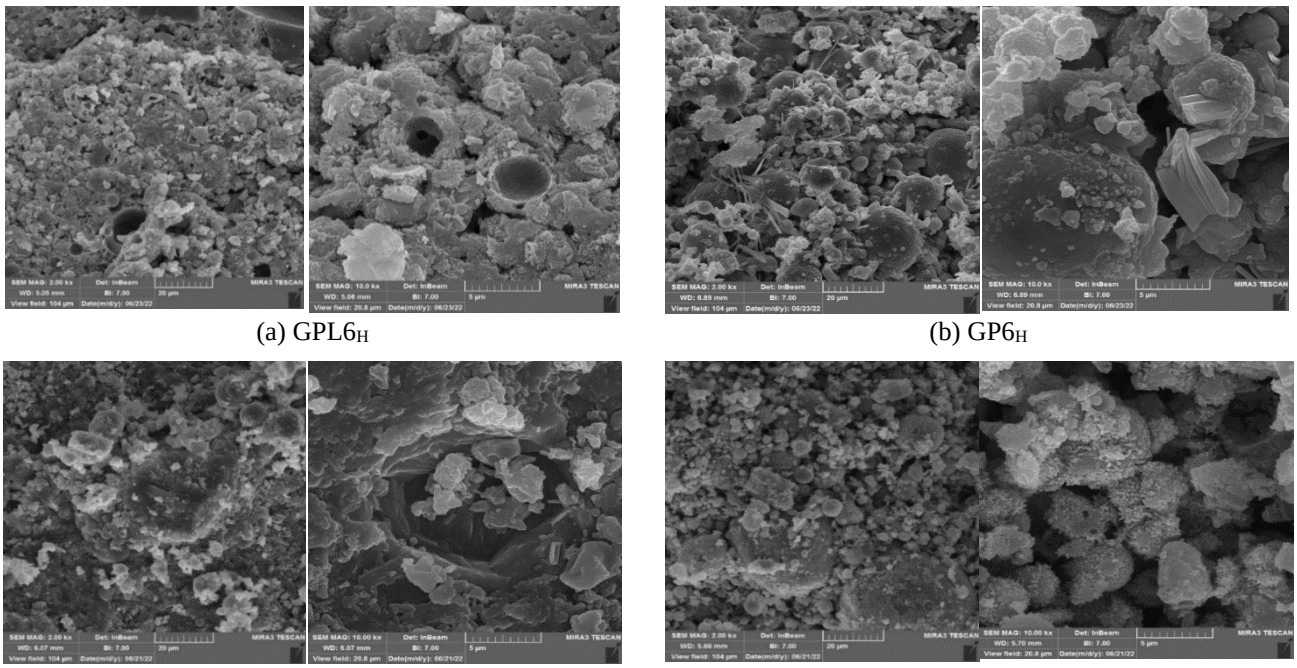

(a) $GPL6_H$ (b) $GP6_H$

(c) $GPL6_R$ (d) $GP6_R$

**Figure 8. SEM Images of a) $GPL6_H$, b) $GP6_H$, c) $GPL6_R$, and d) $GP6_R$ Cured for 90 Days**

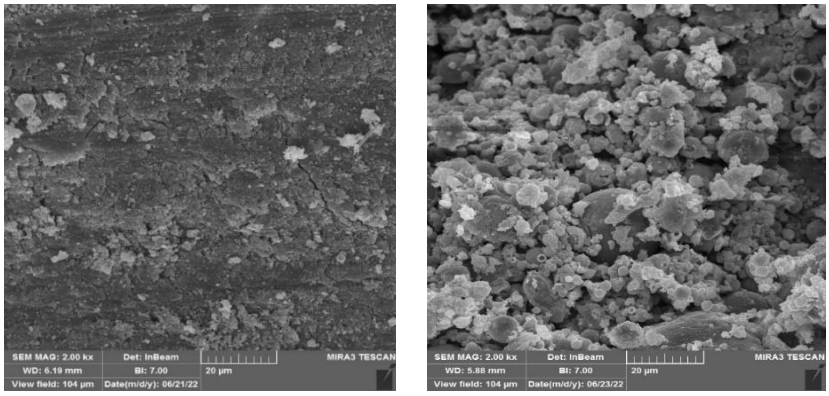


(a) $GPL9_H$ (b) $GPL9_R$

**Figure 9. SEM Images of a) $GPL9_H$, b) $GPL9_R$ Cured for 90 Days**

A comparison between Figures 9a and 8a reveals the low content of unreacted fly ash caused by the low dissolution of fly ash and the reaction products. Furthermore, the morphology presented in Figure 9b showed internal cracking, indicating a weaker matrix compared with the morphology in Figure 8c. These observations confirm the compressive strength test results, in which the samples with 9 M NaOH show a lower UCS than the samples with 6 M NaOH.

## 4. Conclusions

This study evaluate the effects of curing temperature and hydrated lime content on low-alkaline concrete by determining its UCS, modulus of elasticity, and workability. Samples were prepared in two different groups: the specimens of Group 1 were used to determine the optimum hydrated lime content and aging conditions, that is, dry or moist environments for a constant alkali concentration Group 2 was used to assess the mutual effect of different alkali contents. Alkaline solutions with NaOH molarities of 3, 6, and 9 M were then utilized to determine the mutual effect of NaOH molarity and curing temperature, that is, 70 °C for 48 h or room temperature, on the samples with and without hydrated lime. SEM, UCS, modulus of elasticity ($E_{60}$), and workability of the concrete were analyzed to study the effects of curing temperature and hydrated lime content. On the basis of the experimental results and microstructural analyses, the following major conclusions were drawn: (a) An increase in hydrated lime content influences the effect of alkali concentration. UCS exhibited a clear peak for the samples with 6 M NaOH and a continuous rise for the samples without lime. (b) Adding hydrated lime eliminates heat curing and prolonged aging. The samples with 15% hydrated lime and 6 M NaOH cured at room temperature showed a similar UCS to the samples with the same NaOH concentration but without lime and cured at 70 °C. This finding is very beneficial for in-situ concreting and indicates that lime eliminates heat curing to achieve similar UCS. (c) Young's modulus showed a similar trend to UCS, in which $GPL6_H$ showed the maximum value of 28,000 $kg/cm^2$. Only a slight difference in UCS was observed between $GPL6_R$ and $GP6_R$. Therefore, lime reduces the required curing time to reach the UCS of 16,000 $kg/cm^2$, which is very important in filed applications. (d) Similar to the effect of alkali concentration, hydrated lime increases the viscosity of cement, contributing to a loss in slump values. (e) The SEM results were in the line with compressive strength test findings, such that the presence of partially dissolved fly ash in $GPL6_H$ refers to the positive effect of hydrated lime content and heating to dissolve fly ash and increase compressive strength. Moreover, internal cracking contributed to the lower UCS of the samples with 9 M NaOH compared with that of the samples with 6 M NaOH.

## References

[1] J.L. Provis, J.S. Van Deventer (Eds.), Alkali Activated Materials: State-of-the-art Report, RILEM TC 224-AAM, Springer Science Business Media, Berlin, 2014, p.13.
[2] E.K. Najafi, R.J. Chenari, M. Payan, M. Arabani, Bull. Eng. Geol. Environ. 80/5 (2021) 4111.
[3] J. Davidovits, Proceedings of the 1st International Conference on Geopolymer '88, Compiegne, Paris, 1988, p.25.
[4] L. Weng, K. Sagoe-Crentsil, J. Mater. Sci. 42/9 (2007) 2997.
[5] J. Parveen, D. Singhal, M.T. Junaid, B.B. Jindal, A. Mehta, Constr. Build. Mater. 180 (2018) 298.
[6] A.V. Nakum, N.K. Arora, Mater. Today-Proc. 62/6 (2022) 4168.
[7] E.K. Najafi, Adv. Cem. Res. 34/11 (2022) 518.
[8] N. Ranjbar, A. Kashefi, M.R. Maheri, Cement and Concrete Composites, 86 (2018) 8.
[9] H.S. Gökçe, M. Tuyan, K. Ramyar, M.L. Nehdi, J. Mater. Civ. Eng. 32/2 (2020) 04019350.
[10] R.M. Hamidi, Z. Man, L.Z. Azizli, Proc. Eng. 148 (2016) 189-193.

[11] B.S. Gebregziabiher, R.J. Thomas, S. Peethamparan, Constr. Build. Mater. 113 (2016) 783.
[12] F. Nejati, S. Ahmadi, S.A. Edalatpanah, Int. J. Struct. Int. 10/4 (2019) 515.
[13] E. Álvarez-Ayuso, X. Querol, F. Plana, A. Alastuey, N. Moreno, M. Izquierdo, M., *et al*. J. Hazard. Mater. 154/1–3 (2008) 175.
[14] A.H. Aini, H. Masoomi, F. Nejati, J. Basic Appl. Sci. Res. 2/3 (2012) 2405.
[15] A. Hajimohammadi, J.S.J. van Deventer, Int. J. Miner. Process. 153 (2016) 80.
[16] G. Görhan, G. Kürklü, Compos. Part B-Eng. 58 (2014) 371.
[17] S. Moukannaa, M. Loutou, M. Benzaazoua, L. Vitola, J. Alami, R. Hakkou, J. Clean. Prod. 185 (2018) 891.
[18] J. He, W. Bai, W. Zheng, J. He, G. Sang, Constr. Build. Mater. 289 (2021) 123201.
[19] C. Chan, M. Zhang, Constr. Build. Mater. 362 (2023) 129709.
[20] A.M. Rashad, Constr. Build. Mater. 79 (2015) 379.
[21] Specification for Concrete Aggregates, ASTM Standard C33, 2003, West Conshohocken, PA, 2006.
[22] Standard Test Method for Relative Density (Specific Gravity) and Absorption of Fine Aggregate, ASTM Standard C128, West Conshohocken, PA, 2016.
[23] ASTM Standard C127 (2016). "Standard test method for relative density (specific gravity) and absorption of coarse aggregate." West Conshohocken, PA, DOI: 10.1520/C0127-15.
[24] Standard Specification for Coal Fly Ash and Raw or Calcined Natural Pozzolan for use in Concrete, ASTM Standard C168-12a, West Conshohocken, PA, 2012.
[25] Standard Test Method for Slump of Hydraulic Cement Concrete, ASTM C143/C143M-03, West Conshohocken, PA, 2017.
[26] Standard Test Method for Compressive Strength of Cylindrical Concrete Specimens, ASTM C39/C39M, West Conshohocken, PA, 2016.
[27] Pacheco-Torgal, F., Jalali, S., Gomes, J. C. (2009). "Utilization of mining wastes to produce geopolymer binders." "Geopolymers structure, processing, properties and industrial applications," Woodhead Publishing, Sawston, 267-293.
[28] P. Nath, P.K. Sarker, Constr. Build. Mater. 66 (2014) 163.
[29] H. Castillo, H. Collado, T. Droguett, S. Sánchez, M. Vesely, P. Garrido, S. Palma, Minerals. 11/12 (2021) 1317.
[30] C.C. Ban, P.W. Ken, M. Ramli, J. Mater. Civ. Eng. 29/3 (2017) 04016237.
[31] M.Z.N. Khan, F.U.A. Shaikh, Y. Hao, H. Hao, J. Mater. Civ. Eng. 30/2 (2018) 04017267.
[32] S. Song, H.M. Jennings, H. M. (1999). Cement and Concrete Research, 29(2), 159-170.
[33] C.K. Yip, G.C. Lukey, J.L. Provis, J.S.J. Van Deventer, Cement Concrete Res. 38/4 (2008) 554.
[34] T. Phoo-ngernkham, A. Maegawa, N. Mishima, S. Hatanaka, P. Chindaprasirt, Constr. Build. Mater. 91 (2015) 8.
[35] E.L. Mohammadi, E.K. Najafi, P.Z. Ranjbar, M. Payan, R.J. Chenari, B. Fatahi, Constr. Build. Mater. 393 (2023) 132083.
[36] I. García-Lodeiro, O. Maltseva, A. Palomo, Á. Fernández-Jiménez, Rev. Rom. Mater. 42/4 (2012) 330.
[37] M. Zribi, B. Samet, S. Baklouti, J. Non-Cryst. Solids. 511 (2019) 62.
[38] L. Manjarrez, A. Nikvar-Hassani, R. Shadnia, L. Zhang, J. Mater. Civil Eng. 31/8 (2019) 04019156.
[39] Standard specification for loadbearing concrete masonry units, ASTM Standard C90, West Conshohocken, PA, 2011.
[40] National Home Building Registration Council, Annual Report, 2018.
[41] P. Rovnaník, Constr. Build. Mater. 24/7 (2010) 1176.
[42] X. Tian, W. Xu, S. Song, F. Rao, L. Xia, Chemosphere. 253 (2020) 126754.
[43] Standard Test Method for Static Modulus of Elasticity and Poisson's Ratio of Concrete in Compression, ASTM Standard C469, West Conshohocken, PA, 2014.
[44] K.H. Yang, J.K. Song, J. Mater. Civil Eng. 21/3 (2009) 119.
[45] B. Walkley, R. San Nicolas, M.A. Sani, G.J. Rees, J.V. Hanna, J.S.J. van Deventer, J.L. Provis, Cement Concrete Res. 89 (2016) 120.
[46] J. Yang, D. Li, Y. Fang, Materials. 10/7 (2017) 695.
[47] F. Nejati, M. Hosseini, A. Mahmoudzadeh, Int. J. Struct. Integ. 8/3 (2017) 326.